J Therm Anal Calorim (2012) 110:707–713
DOI 10.1007/s10973-011-1919-5

Pyrolysis mechanism of trisbipyridineiron(II) chloride to iron nanoparticles

Rabia Nazir · Muhammad Mazhar · Tehmina Wakeel · Muhammad J. Akhtar · Muhammad Siddique · Muhammad Nadeem · Nawazish A. Khan · Muhammad R. Shah

Received: 2 July 2011 / Accepted: 13 September 2011 / Published online: 30 September 2011

Abstract Pyrolysis of trisbipyridineiron(II) chloride under controlled thermal conditions and inert atmosphere of argon gas yields a residue of iron nanoparticles. Evolved gas analysis by GC–MS and ^{1}H NMR revealed emission of bipyridine, 6-chlorobipyridine, 6,6′-dichlorbipyridine, bipyridine hydrochloride, and hydrochloric acid as decomposition products. CHN, XRPD, EDXRF, TEM, AFM, and ^{57}Fe Mössbauer spectroscopy of the residue indicated formation of pure iron nanoparticles in the size range of 50–72 nm. Based on these results a mechanism for thermal degradation of trisbipyridineiron(II) chloride has been worked out.

R. Nazir · T. Wakeel
Department of Chemistry, Quaid-i-Azam University, Islamabad 45320, Pakistan

R. Nazir
Applied Chemistry Research Centre, Pakistan Council of Scientific and Industrial Research Laboratories Complex, Lahore 54600, Pakistan

M. Mazhar (✉)
Department of Chemistry, University of Malaya, Lembah Pantai, 50603 Kuala Lumpur, Malaysia
e-mail: mazhar42pk@yahoo.com

M. J. Akhtar · M. Siddique · M. Nadeem
Physics Division, PINSTECH, P.O. Nilore, Islamabad, Pakistan

N. A. Khan
Material Science Laboratory, Department of Physics, Quaid-i-Azam University, Islamabad 45320, Pakistan

M. R. Shah
HEJ Research Institute of Chemistry, University of Karachi, Karachi 75270, Pakistan

Keywords Trisbipyridineiron(II) chloride · Pyrolysis · Iron nanoparticles · Mechanism

Introduction

Metal bipyridine complexes have played an important role in many areas of life ranging from simple analytical determinations [1, 2] to as complex as part of human DNA strand [3, 4]. The ease of synthesis and stability of these complexes makes them very interesting materials to be studied. Although, several researchers investigated stability and thermal decomposition of metal bipyridine complexes and various mechanisms have also been proposed [5–18] but still there remains quite a contradiction related to their final thermolysis products.

Thermal decomposition of MLX (where $L = 2,2'$-bipy) type complexes in the presence of air resulted in respective metal oxide or zero-valent metal, in cases where X = SCN [5] and if X = oxalate the probable final degradation products were always respective metals' oxides [6, 7]. Metal oxides formation is also reported as a result of thermal decomposition in the presence of air in complexes where X is di- or tri-choloracetate [8–11] or propionates [12] and L = different isomers of bipyridine, via several intermediates, while in case of transition metal nitrates of 2,2′-bipy, metal oxide formation takes place in the presence of inert atmosphere [13]. In bipyridine complexes thermal degradation depends on the type of metal, bipyridine ligand, and heating rates, the stability order follows as 2,2′-bipy > 4,4′-bipy > 2,4′-bipy. The higher stability of 2,2′-bipy is attributed to its ability to form five membered ring [6]. In dimeric complexes of type $[Ln(CA)_3bipy]_2$ (where Ln = Tb and Dy; CA = cinnamic acid), the thermal

decomposition took place by elimination of bipyridine and acid ligand to result in metal oxide [14]. In case of W(2,2′-bipy)Cl_4 complex, complete thermal decomposition resulted in the formation of tungsten carbide under argon atmosphere in the presence of excess of 2,2′-bipy. The zero-valent metal formation also took place in samples where 2,2′-bipy is present in small amounts owing to its evaporation during heating before decomposition [15]. Stepwise controlled thermal decomposition of the [Ni(bipy)$_3$]Cl_2·7H_2O and [Co(bipy)$_3$]Cl_2·H_2O up to 270 °C had resulted in compounds of the following formulas: M(bipy)$_2Cl_2$, M$_3$(bipy)$_4Cl_6$, Ni(bipy)Cl_2, isomeric Co(bipy)Cl_2, Co(bipy)$_{0.80}Cl_2$, and M(bipy)$_{0.50}Cl_2$ but failed to get the Ni(bipy)$_{1.50}Br_2$ analog of chloride [16] as was earlier reported by Dhar and Baslao [17] for thermal decomposition of [Ni(bipy)$_3$]Br_2·7H_2O. This difference in decomposition patterns was attributed to the presence of different anions [17]. [Rh(bipy)$_3$]$^{+3}$, on other hand, decomposed to metallic Rh irrespective of the type of halide atom present [18]. No constant pattern of thermal decomposition was observed in case of [M(bipy)$_3$]Br_2 where M = Mn(II), Co(II), and Zn(II) [17]. Further studies on Co(bipy)Cl_2·HCl, Co(bipy)Cl_2·H_2O, and Co(bipy)Cl_2 were also carried out that showed initial loss of HCl and water prior to being decomposed oxidatively in air atmosphere around 380 °C. Same pattern was observed for Ni(bipy)Cl_2 [19] but the decomposition of hydrated and anhydrous complexes were found to show different thermal decomposition patterns at different temperatures [20].

Hence, considering the importance of bipyridine complexes, present study was initiated with aim to re-evaluate the thermal decomposition pattern of the bipyridine complexes. We focused our investigations on mechanism of pyrolysis of anhydrous trisbipyridineiron(II) chloride under controlled temperature and ambient pressure and characterization of the residual mass and found that the complex degrades to iron nanoparticles under given conditions. Thus, prepared iron nanoparticles may find various technological applications in field of catalysis [21, 22], electrolysis [23], energy [24], biomedicine [25], and environment [26–28]. To the best of our knowledge this mode of decomposition of trisbipyridineiron(II) chloride under controlled thermal and ambient pressure has not been reported before.

Experimental details

Materials

All the reagents used were of analytical grade while ferrous chloride tetrahydrate was purchased from Merck and 2,2′-bipyridine from Sigma-Aldrich.

Synthesis

[Fe(bipy)$_3$]Cl_2

1.98 g (10 mmoles) of $FeCl_2$·4H_2O in 100 mL dried THF was placed in a 250 mL three-necked round-bottom flask fitted with a reflux condenser, a dropping funnel and an inert gas line. 4.70 g (30 mol) of 2,2′-bipyridine in 50 mL of dried THF was slowly added to the reaction flask from a dropping funnel over a period of 24 h with continuous stirring of the contents during addition. Yellow precipitates formed were filtered through a sintered glass crucible and washed several times with THF to remove the reactants. The product was crystallized from methanol at room temperature to give 80–86% yield [29]. m.p. = 168 °C; λ_{max} (H_2O) 520 nm, IR (KBr, cm^{-1}): ν(C-H$_{arom}$) 3050, 2927; ν(C-N$_{arom}$) 1599; ν(C-C$_{arom}$) 1493, 1443, 900-600; ν(Fe–N) 416. ^{1}H NMR (DMSO, ppm): 8.440 (s, 6H, bipyH$_{6,6'}$); 8.220 (s, 6H, bipyH$_{3,3'}$); 7.797 (s, 6H, bipyH$_{4,4'}$); 7.299 (s, 6H, bipyH$_{5,5'}$). FAB: [M − L−HCl]$^+$*m/z* 403, [FeL$_2$]$^+$ *m/z* 368, [FeLCl]$^+$ *m/z* 247, [FeL]$^+$ *m/z* 212, [L + 1]$^+$ *m/z* 157.

Characterization

The bipyridine complex was analyzed using a Perkin Elmer Spectrophotometer, Nicolet 6700 FT-IR, Bruker 300 MHz NMR, and Mettler Toledo 851e TGA and DSC404C. FAB analysis was performed using xenon gas and glycerol as matrix. Agilent GC–MS model 6890 N was used for evolved gas analysis. Carbolite furnace was used for thermally decomposing the complex. The prepared samples were characterized by EDXRF using Horiba XRF Analyzer Mensa Bio100, Japan. The powder XRD data were collected, on a Bruker D8 discover, Germany, at room temperature by step scanning over the angular range of $3\mathring{0} \leq 2\theta \leq 8\mathring{0}$ at a step size of $0.0\mathring{5}$ and counting time of 6 s/step. Transmission electron microscopy (TEM) JEOL 2010, operating at 200 kV and atomic force microscopy (AFM), Multimode, NanoscopeIIIa, Veeco, California, USA) in tapping mode were used to analyze size and shape of particles. Dispersion of samples in ethanol was spin coated on freshly cleaved sheet of mica substrate. AFM images were acquired at room temperature and repeated several times with different concentrations of samples. Silicon cantilevers (Nanoworld, Switzerland; 240 μm long, 30 μm wide, 2.8 μm thick) with an integrated tip, a nominal spring constant of 0.7–3.8 N/m, tip radius <10 nm and a resonance frequency of 70 kHz were plasma cleaned before use use. A piezoelectric scanner (Veeco Instruments, California, USA) with a maximum *x*, *y*-scan range of 17.2 μm and a *z*-extension of 3.916 μm was used. Typically the tip was scanned at velocity from 0.5 to 1 μms^{-1}. Topography, phase and height images were used

to record the structures. Raw data were modified by applying the first order 'flatten' filter in order to achieve scan lines at the same average height and tilt. Room temperature Mössbauer measurements were carried out using a ^{57}Co (Rh-matrix) source, having 25 mCi initial activity, in transmission geometry. The computer program Mos-90 was used for performing data analysis assuming that all the peaks are of Lorentzian shape [30].

Results and discussion

Anhydrous trisbipyridineiron(II) chloride was prepared in quantitative yield by the method developed by Basalo [31] except using dry THF in place of water as a solvent to avoid association of H_2O with the complex in the form of ligand or as a solvate. Thus, the prepared complex was crystallized from anhydrous methanol and characterized by melting point, UV/VIS, FT-IR, ^{1}H NMR, and mass spectrometry. All the analytical data of the complex matches well with the reported values [32, 33]. The complex shows λ_{max} at 520 nm which is very close to the reported value of 522 nm [34, 35].The Mössbauer spectrum of the complex consists of a doublet having an isomer shift of 0.34 mm/s and a quadrupole splitting of 0.24 mm/s which are in close agreement with the reported values, i.e., 0.33 and 0.28 mm/s, respectively [34, 35].

Different pyrolysis experiments on $[Fe(bipy)_3]Cl_2$ were conducted in a tube furnace using an open and closed vessel under varying argon gas flow rates while keeping heating rate of 0.5 °C/min constant and it was found that in a closed vessel and under low gas flow rate, the residue had appreciable amount of iron contaminated with degraded mass consisting of carbon, hydrogen, nitrogen, and chlorine. It was observed that when gas flow rate was increased from 30 mL/min to 2L/min in an open vessel the complex degraded quantitatively to yield a residue of pure shiny black residue that was later characterized by various analytical techniques as iron nanoparticles. The effect of argon gas flow rate on the quality of the residue was also investigated by thermogravimetric studies and it was observed that low flow rate of 50 mL/min yields a residue of 24.65% while increasing the rate to 250 mL/min produced 14.83% residue. CHN analyses of both the residues obtained under low and high flow rates are presented in Table 1.

Figure 1a shows that $FeCl_2{\cdot}4H_2O$ decomposes in two stages with % mass loss of 43.81% in first step probably owing to loss of two water molecules and one HCl molecule (giving 45.72% calculated value) and 17.64% in second step giving residue of 34.32% which suggests formation of mixture of FeO and Fe (calculated value 36.18%) as end product which remains stable up to 1000 °C. Bipyridine evaporates almost completely in a single step at 225 °C with a residual mass of 2.29%. Thermogram of the complex (Fig. 1b) shows that the complex passes through different complex stages of pyrolysis to yield a residual mass of 14.88% that resembles closely to % age of iron in the complex. It is further observed that the decomposition temperatures are significantly delayed due to the high flow rate of carrier gas [38–40].

Table 1 Elemental analysis of the residues showing effect of argon gas flow rate, increase in temperature and type of vessel on the pyrolysis residue of $[Fe(bipy)_3]Cl_2$

Experimental conditions		Elemental analysis of residues			
Heating vessel; Gas flow rate	Heating temperature/°C	C/%	H/%	N/%	Cl/wt%
Closed; 30 mL/min	450	24.98	1.69	8.92	19.28
Open; 2 L/min	450	1.80	0.05	1.05	–
Closed; 30 mL/min	600	32.68	1.97	7.41	13.50
Open; 2L/min	600	0.027	–	0.154	–

Earlier thermogravimetric studies by Sato et al. [36, 37] on hydrated $[Fe(bipy)_3]Cl_2{\cdot}5H_2O$ complex showed its four step decomposition to $FeCl_2$ with the release of water and bipyridine in different stages of decomposition. Our TG studies on anhydrous trisbipyridineiron(II) chloride indicated formation of iron particles rather than stable $FeCl_2$ residue, as previously reported by Sato and Tominaga [36, 37]. To solve this obvious contradiction we carried out several pyrolysis experiments in tube furnace under identical conditions that were used in TG recording. The evolved gases from exhaust of the tube furnace were trapped in a clean pre-evacuated Schlenk tube for GC–MS and ^{1}H NMR studies that showed without any shadow of doubt, emission of bipyridine, chlorobipyridine, dichloropyidine, bipyridine hydrochloride, and hydrochloric acid as pyrolysis byproducts.

The evolved gases were found to contain bipyridine as a major constituent. The bipyridine recovered (bipy-r) from the trap after decomposition was subjected to various analysis for confirmation and close resemblance was observed between bipy-r and the pure bipyridine (bipy). Comparative account of bipy and bipy-r is presented in Table 2. Small difference that arises between these two especially in the percentage weight residue is due to the presence of impurities in the recovered bipyridine. The emission of bipyridine was also confirmed by GC–MS analysis of the evolved gas collected from the thermal degradation of $[Fe(bipy)_3]Cl_2$ at different intervals of time which showed a peak having retention time (R_t) of 5.9 min with m/z value of 156 confirming the presence of bipyridine that appeared in all the collected samples. Few other peaks were also observed in

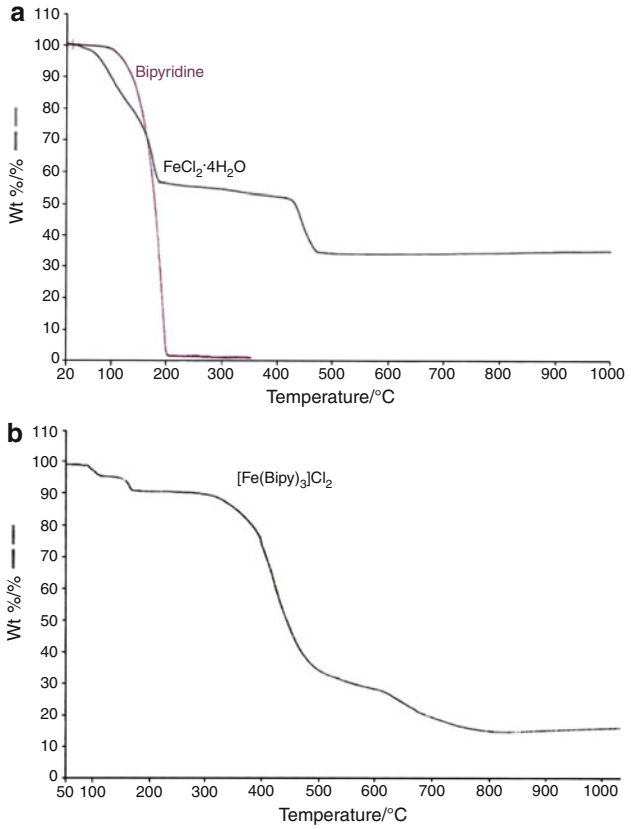

Fig. 1 Thermograms of **a** $FeCl_2{\cdot}4H_2O$ and bipyridine at heating rate of 20 °C/min and gas flow rate of 200 mL/min, **b** $[Fe(bipy)_3]Cl_2$ at heating rate of 5 °C/min and gas flow rate of 250 mL/min

the chromatogram, which were identified by their mass spectra. A peak having *m/z* of 191 appearing at R_t of 6.3 min denotes the presence of bipyridine hydrochloride. Two more peaks recorded in GC at R_t 7.7 and 7.9 min having *m/z* value of 190 showed the presence of two different isomeric chlorobipyridines. Analysis of the crystalline solid recovered from the ethanol trap showed one more peak with R_t of 7.2 min and *m/z* of 224 which indicated the formation of 6,6′-dichlorobipyridine.

The solid condensate trapped was fractionated to individual components by crystallization in appropriate solvents and was subjected to ^{1}H NMR and the data confirms the formation of chlorobipyridine.

^{1}H NMR-chlorobipy (CD_3OD, ppm): 8.926–8.910 (m, 1H, $bipyH_3$); 8.770–8.744 (m, 1H, $bipyH_{3'}$); 8.667–8.640 (m, 1H, $bipyH_{6'}$); 8.509–8.452 (m, 1H, $bipyH_5$); 8.205 (m, 1H, $bipyH_{5'}$); 7.963–7.922 (m, 1H, $bipyH_4$); 7.252–7.505 (m, 1H, $bipyH_{4'}$).

Based on our observations and earlier studies [41, 42] on the thermal degradation of $[Fe(bipy)_3]Cl_2$, a mechanism (Scheme 1) has been proposed for the thermal degradation of $[Fe(bipy)_3]Cl_2$ to iron residue. The elimination of bipyridine in initial two steps induces coordinative unsaturation on the iron centre paving the way for H-abstraction from pyridine ring followed by reductive elimination to finally yield iron nanoparticles.

The residual shiny black mass obtained after the thermal decomposition of $[Fe(bipy)_3]Cl_2$ was subjected to elemental analysis, EDXRF, XRPD, AFM, TEM, and ^{57}Fe Mössbauer spectroscopy for its characterization. CHN analysis showed little contamination of carbon and nitrogen (Table 1) while EDXRF provided evidence for the absence of chlorine and the revealed emission is exclusively due to iron atom within the detection limit of experiment. XRPD spectra (not shown here) of the sample annealed at 1000 °C showed a peak at 2θ value of 45° indicating the formation of iron in a *bcc* phase [43]. AFM and TEM images (Fig. 2) show homogeneously dispersed spherical shaped nanoparticles with well-defined grain boundaries in the size ranges of 50–72 nm.

Further characterization of the iron nanoparticles was carried out by ^{57}Fe Mössbauer spectroscopy. The ^{57}Fe Mössbauer spectrum for the sample, shown in Fig. 3, consists of a paramagnetic doublet instead of a typical ferromagnetic sextet as in the case of bulk iron confirming the formation of iron nanoparticles [44]. This doublet is due to the evolution of size-dependent paramagnetism when size is reduced to nanoscale [44]. Mössbauer

Table 2 Comparative account of pure bipyridine (bipy) and the one recovered from trap after decomposition of the $[Fe(bipy)_3]Cl_2$ complex (bipy-r)

FT-IR			^{1}H NMR			TG		
ν/cm^{-1}	bipy	bipy-r	δ/ppm	bipy	bipy-r		bipy	bipy-r
(C-H_{arom})	3070	3075	(m, 2H, $bipyH_{6,6'}$)	8.682–8.666	9.062–9.941	Wt.% of residue	0.60%	3.34%
	3028	2927						
(C-N_{arom})	1061	1602	(m, 2H, $bipyH_{3,3'}$)	8.402–8.376	8.303	Temp.	199 °C	177 °C
(C-C_{arom})	1493	1490	(m, 2H, $bipyH_{4,4'}$)	7.829–7.771	7.758			
	1451	1499						
	600	900–600						
			(m, 2H, $bipyH_{5,5'}$)	7.311–7.267	7.281			

Scheme 1 Mechanism of thermal decomposition of $[Fe(bipy)_3]Cl_2$ to Fe (0) under inert atmosphere

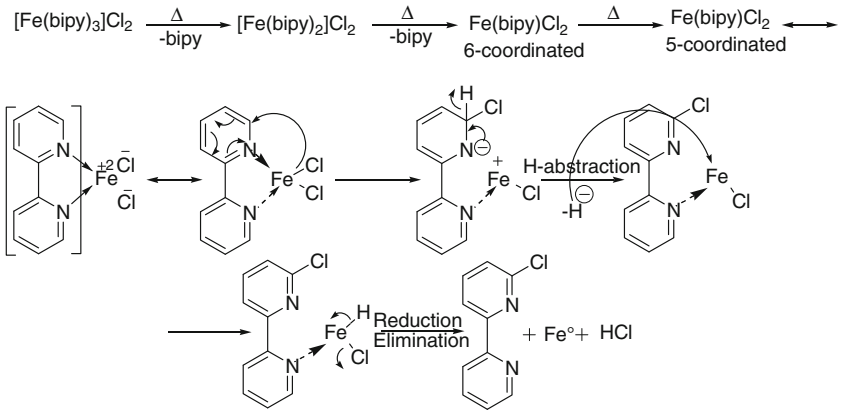

Fig. 2 **a** AFM image, **b** section analysis of AFM, and **c** TEM image of iron nanoparticles obtained from pyrolysis of $[Fe(bipy)_3]Cl_2$

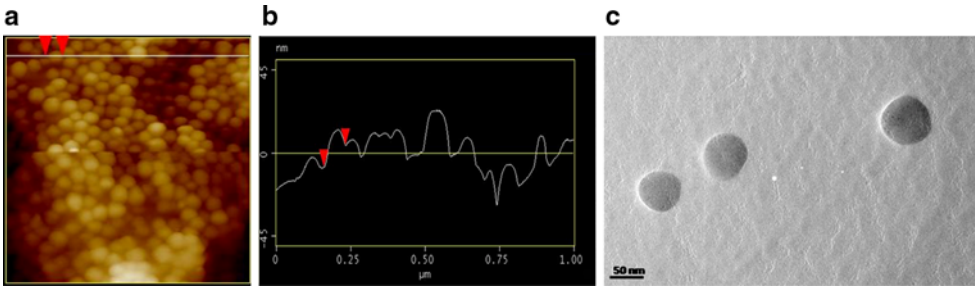

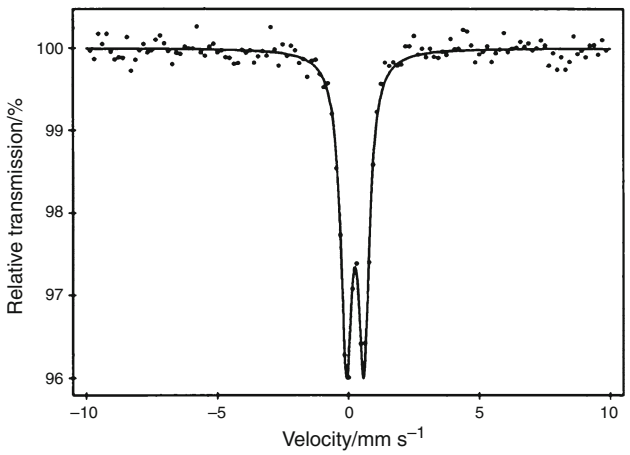

Fig. 3 ^{57}Fe Mössbauer spectrum for iron nanoparticles obtained from pyrolysis of $[Fe(bipy)_3]Cl_2$ showing superparamagnetic doublet

parameters for the doublet, i.e., isomer shift, quadruple splitting, and line width are 0.29, 0.69, and 0.65 mm/s, respectively, confirming formation of iron nanoparticles.

Hence, from the forgone discussion it can be inferred that thermal decomposition of trisbipyridineiron(II) chloride under controlled conditions leads to the formation of pure iron nanoparticles. This method of preparation of iron nanoparticles offers an easy, simple, and cost effective approach to their preparation as compared to the other methods that either use toxic reactants [45] and/or require use of various measures that enable them to protect the nanoparticles from oxidation [46, 47].

Conclusions

It is concluded that anhydrous trisbipyridineiron(II) chloride thermally degrades in an open vessel under controlled heating and argon gas flow rates to yield iron nanoparticles residue. A mechanism of thermal degradation based on evolved gas analysis has been worked out. The resulting final thermolysis product was analyzed using CHN, ED-XRF, XPRD, AFM, TEM, and Mössbauer spectroscopy which confirmed the formation of *bcc* iron nanoparticles with size ranging from 50 to 72 nm as end product.

Acknowledgements RN and MM acknowledge the Higher Education Commission of Pakistan for financial support through indigenous scholarship scheme for Ph.D. studies in science and technology (300 Sch.), HEC project no. 1-308/ILPUFU/HEC/2009- and HIR/UMRG grant no.UM.C/625/1/1/6 and RG097110AET of University of Malaya.

References

1. Mehlig JP, Koehmstedt PL. Spectrophotometric determination of copper in ores with 2, 2′-bipyridine. Anal Chem. 1953;25:1920–1.
2. Koeing RA, Johnson CR. Spectrophotometric determination of iron: II use of 2,2′-bipyridine. J Biol Chem. 1942;143:159–63.
3. Rodriquez-Ramos MM, Wilker JJ, Boil J. Metal bipyridine complexes in DNA backbones and effect on thermal stability. Inorg Chem. 2010;15:629–39.
4. Weizman H, Tor Y. 2,2′-bipyridine lignoside: a novel building block for modifying DNA with intra-duplex metal complexes. J Am Chem Soc. 2001;123:3375–6.

5. Czakis-Sulikowska D, Kaluzna J, Radwańska-Doczekalska J. Thermal studies of new Cu(I) and Ag(I) complexes with bipyridine isomers. J Therm Anal. 1998;54:103–13.
6. Czakis-Sulikowska D, Malinowska A, Markiewicz M. Synthesis and thermal decomposition of new complexes of bipyridine isomers with Zn(II) and Cd(II) oxalates. J Therm Anal Colorim. 2000;60:151–6.
7. Czakis-Sulikowska D, Kaluzna J, Radwańska-Doczekalska J. Synthesis, properties and thermal decomposition of bipyridine-oxalato complexes with Mn(II), Co(II), Ni(II) and Cu(II). Polish J Chem. 2000;74:607–14.
8. Czakis-Sulikowska D, Czylkowska A. Thermal and other properties of complexes of Mn(II), Co (II) and Ni(II) with 2,2′-bipyridine and trichloroacetates. J Therm Anal Colorim. 2003;74:349–60.
9. Czakis-Sulikowska D, Czylkowska A. Complexes of Mn(II), Co (II), Ni(II) and Cu(II) with 4,4′-bipyridine and dichloroacetates. J Therm Anal Colorim. 2003;71:395–405.
10. Czylkowska A, Markiewicz M. Coordination behavior and thermolysis of some rare-earth complexes with 4,4′-bipyridine and di- or trichloroacetates. J Therm Anal Colorim. 2010;100:717–23.
11. Czylkowska A, Czakis-Sulikowska D, Kaczmarek A, Markiewicz M. Thermal behavior and other properties of Pr(III), Sm(III), Eu(III), Gd(III), Tb(III) complexes with 4,4′-bipyridine and trichloroacetates. J Therm Anal Colorim. 2011;105:331–9.
12. Czakis-Sulikowska D, Radwańska-Doczekalska J, Markiewicz M, Pietrzak M. Thermal characterization of new complexes of Zn(II) and Cd(II) with some bipyridine isomers and propionates. J Therm Anal Colorim. 2008;93:789–94.
13. Kumar D, Kapoor IPS, Singh G, Geol N, Singh UP. Preparation, X-ray crystallography and thermolysis of transition metal nitrates of 2,2′-bipyridine (Part 63). J Therm Anal Colorim. 2011. doi: 10.1007/s10973-011-1781-5.
14. Tian L, Ren N, Zhang JJ, Liu HM, Sun SJ, Ye HM, Wu KZ. Synthesis and thermal decomposition kinetics of two lanthanide complexes with cinnamic acid and 2,2′-bipyridine. J Therm Anal Colorim. 2010;99:349–56.
15. Wanner S, Hilaire L, Wehrer P, Hindermann JP, Maire G. Obtaining tungsten bipyridine complexes via low temperature thermal treatment. Appl Catal A-Gen. 2000;203:55–70.
16. Lee RH, Griwold E, Kleinberg J. Studies on the stepwise controlled decomposition of 2,2′-bipyridine complexes of Co(II) and Ni(II) chlorides. Inorg Chem. 1964;3:1278–83.
17. Dhar SK, Basolo F. Thermal decomposition of the tris(2,2′-bipyridine) complexes of some first row transition group elements in the solid state. J Inorg Nucl Chem. 1963;25:37–44.
18. Bujewski A, Walewski M, Grzedzicki K. Synthesis and thermal investigations of [Rh(bpy)3]X3, (bpy = 2,2′-dipyridyl; X = Cl-, Br-, I-, ReO4- and [M(bpy)3][CdnX2n + 3] (X = Cl-, Br-, I-) type complexes. Thermochim Acta. 1991;185:91–8.
19. Akabori K, Matsuo H, Yamamoto Y. Thermal properties of mono(2,2′-bipyrinde)cobalt(II) and nickel(II) chloride. J Inorg Nucl Chem. 1971;33:2593–601.
20. Czakis-Sulikowska D, Kałużna-Czaplińska J. Thermal properties of complexes of Mn(II), Fe(II), Co(II), Ni(II) with 2,2′-bipyridine or 4,4-bipyridine and thiocyanates. J Therm Anal Colorim. 2000;62:821–30.
21. Guo L, Huang Q, Li X, Yang S. Iron nanoparticles: synthesis and applications in surface enhanced Raman scattering and electrocatalysis. Phys Chem Chem Phys. 2001;3:1661–5.
22. Yang Y, Liu X, Guo X, Xu B. Synthesis of nano onion-like fullerenes by chemical vapor deposition using an iron catalyst supported on sodium chloride. J Nanopart Res. 2011;13:1979–86.
23. Huang K, Chou K. Microstructure changes to iron nanoparticles during discharge/charge cycles. Electrochem Commun. 2007;9:1907–12.
24. Beach DB, Rondinone AJ, Sumpter BG, Labinov SD, Richard RK. Solid-state combustion of metallic nanoparticles: new possibilities for alternative energy carrier. J Energy Res Technol. 2007;129:29–32.
25. Šafařík I, Horská K, Šafaříková M. Magnetic nanoparticles for biomedicine. Fundamental Biomedical Technologies. 2011;5:363–72.
26. Najaa G, Apiratikula R, Pavasante P, Voleskya B, Hawari J. Dynamic and equilibrium studies of the RDX removal from soil using CMC-coated zerovalent iron nanoparticles. Environ Pollut. 2009;157:2405–12.
27. Elliott DW, Lien H, Zhang W. Degradation of lindane by zerovalent iron nanoparticles. J Environ Eng. 2009;135:317–24.
28. Zhang D, Wei S, Kaila C, Su X, Wu J, Karki AB, Young DP, Guo Z. Carbon-stabilized iron nanoparticles for environmental remediation. Nanoscale. 2010;2:917–9.
29. Nazir R, Mazhar M, Siddique M, Hussain ST. Effect of particle size and alloying with different metals on ^{57}Fe Mossbauer spectra. Hyperfine Interact. 2009;189:85–9.
30. Groβe G Mos-90 Version 2.2 Manual and program. Documentation 2nd ed. March 1992.
31. Basalo F, Johnson R. Preparations and reactions of coordination compounds. In: Johnson R, editor. Coordination chemistry, the chemistry of metal complexes. New York: Benjamin Inc.; 1964.
32. Inskeep RG. Infra-red spectra of metal complex ions below 600 cm^{-1}: The spectra of the tris complexes of 1,10-phenanthroline and 2,2′-bipyridine with transition metals iron (II) through zinc (II). J Inorg Nucl Chem. 1962;24:763–76.
33. Miller JM, Balasanmugam K. Characterization of metal complexes of 1,10-phenanthroline, 2, 2′-bipyridine and their derivatives by fast atomic spectrometry. Can J Chem. 1989;67:1496–500.
34. Charlet GR. Colorimetric determination of elements. New York: Elsevier Science Ltd.; 1989.
35. Nakanishi C, Saorilkeda, Isobe T, Senna M. Silica- $[Fe(bpy)_3]^{2+}$ composite particles with photo-responsive change of color and magnetic property. Mater Res Bull. 2002;37:647–51.
36. Sato H, Tominaga T. Mössbauer studies of the thermal decomposition of tris(2,2′-bipyridine)iron(II) chloride and the structure of the isomers of 2,2′-bipyridineiron(II) chloride. Bull Chem Soc Jpn. 1976;49:697–700.
37. Sato H, Tominaga T. A Mössbauer study on the thermal decomposition of tris(2,2′-bipyridine)iron(II) chloride. Radiochem Radioanal Lett. 1975;22:3–10.
38. Keuleers R, Janssen J, Desseyn HO. Instrument dependence and influence of heating rate, mass, ΔH, purge gas and flow rate on the difference between experimental and programmed temperature of the instrument. Thermochim Acta. 1999;333:67–71.
39. Reich L, Patel SH, Stivala SS. Factors affecting the thermal decomposition of cadmium carbonate by TG. Thermochim Acta. 1989;138:147–60.
40. Berbenni V, Marini A, Bruni G, Zerlia T. TG/FTIR: an analysis of the conditions affecting the combined TG/spectral response. Thermochim Acta. 1995;258:125–33.
41. Reiff WM, Dockum B, Weber MA, Frankel RB. Magnetic ordering of mono(diimine)iron(II) chlorides, (2,2′-bipyridine)dichloroiron and (5,5′-dimethyl-2,2′-bipyridine)dichloroiron. Inorg Chem. 1975;14:800–6.
42. Reiff WM, Long GJ. Mössbauer spectroscopy and coordination chemistry of iron. In: Long GJ, editor. Mössbauer spectroscopy applied to inorganic chemistry, vol. 1. New York: Plenum Press; 1984. p. 245–9.

43. Choi CJ, Dong XL, Kim BK. Characterization of Fe and Co nanoparticles synthesized by chemical vapor condensation. Scr Mater. 2001;44:2225–9.
44. Sen P, Ghosh J, Abdullah A, Kumar P. Preparation of Cu, Ag, Fe and Al nanoparticles by exploding wire technique Vandana. Proc Indian Acad Sci (Chem Sci). 2003;115:499–508.
45. Shao H, Lee H, Huang Y, Ko I, Kim C. Control of iron nanoparticles size and shape by thermal decomposition method. IEEE Trans Magn. 2005;41:3388–90.
46. He Y, Sahoo Y, Wang S, Luo H, Prasad PN, Swihart MT. Laser-driven synthesis and magnetic properties of iron nanoparticles. J Nanopart Res. 2006;8:335–42.
47. Laurent S, Forge D, Port M, Roch A, Robic C, Elst LV, Muller RN. Magnetic iron oxide nanoparticles: synthesis, stabilization, vectorization, physiochemical characterization and biological applications. Chem Rev. 2008;108:2064–110.